Oxidation of Methionine Residues in Recombinant Human Interleukin-1 Receptor Antagonist: Implications of Conformational Stability on Protein Oxidation Kinetics[†]

Renuka Thirumangalathu,[‡] Sampathkumar Krishnan,*[,§] Pavel Bondarenko,[§] Margaret Speed-Ricci,[§] Theodore W. Randolph,[||] John F. Carpenter,[‡] and David N. Brems*[,§]

Center for Pharmaceutical Biotechnology, Department of Pharmaceutical Sciences, University of Colorado Health Sciences Center, Denver, Colorado 80262, Department of Pharmaceutics, Amgen Inc., Thousand Oaks, California 91320, and Department of Chemical and Biological Engineering, University of Colorado, Boulder, Colorado 80309

Received February 14, 2007; Revised Manuscript Received March 9, 2007

ABSTRACT: Oxidation of methionine residues is involved in several biochemical processes and in degradation of therapeutic proteins. The relationship between conformational stability and methionine oxidation in recombinant human interleukin-1 receptor antagonist (rhIL-1ra) was investigated to document how thermodynamics of unfolding affect methionine oxidation in proteins. Conformational stability of rhIL-1ra was monitored by equilibrium urea denaturation, and thermodynamic parameters of unfolding (ΔG_{H2O}, m, and C_m) were estimated at different temperatures. Methionine oxidation induced by hydrogen peroxide at varying temperatures was monitored during "coincubation" of rhIL-1ra with peptides mimicking specific regions of the reactive methionine residues in the protein. The coincubation study allowed estimation of oxidation rates in protein and peptide at each temperature from which normalized oxidation rate constants and activation energies were calculated. The rate constants for buried Met-11 in the protein were lower than for methionine in the peptide with an associated increase in activation energy. The rate constants and activation energy of solvent exposed methionines in protein and peptide were similar. The results showed that conformational stability, monitored using the C_m value, has an effect on oxidation rates of buried methionines. The rate constant of buried Met-11 correlated well with the C_m value but not ΔG_{H2O}. No correlation was observed for the oxidation rates of solvent-exposed methionines with any thermodynamic parameters of unfolding. The findings presented have implications in protein engineering, in design of accelerated stability studies for protein formulation development, and in understanding disease conditions involving protein oxidation.

Protein methionine (Met[1]) oxidation is a predominant degradation pathway of proteins with both structural and functional consequences. Control of Met oxidation in protein pharmaceuticals continues to be a critical issue in developing stable formulations (*1*). The biological activity of proteins can be significantly affected, with complete loss of functionality upon oxidation of Met to methionine sulfoxide (MetSO) or sulfones. Some examples of proteins that show decreased activity upon Met oxidation include but are not limited to calmodulin (*2*); α1-protease inhibitor (*3*); human chorionic somatotropin (*4*); subtilisin (*5*); and recombinant human granulocyte colony stimulating factor (*6*). Met oxidation in thrombodulin disrupts its structure with consequent loss of anticoagulant activity (*7*). Furthermore, Met oxidation was found to increase during aging and has been associated with inflammatory diseases, neurologic disorders, and cataractogenesis (*8*−*10*). Therefore, it is of importance to understand the factors modulating Met oxidation in proteins and thus rationalize strategies to counter this process in vitro and in vivo.

Evidence in the literature points to the conformational control of Met oxidation in proteins. For example, surface accessibility or the lack of it can strongly modulate the oxidation rates of Met residues in proteins (*4*−*6*, *11*−*13*). If a Met residue is significantly surface exposed, it shows greater tendency to be oxidized compared to a partially or a fully buried residue in the interior of the protein. Hence, Met oxidation has been typically correlated with the solvent-accessible area (SAA) of these residues in protein. More recently, Chu et al. (*14*) have proposed the "water-mediated" mechanism for Met oxidation in recombinant human granulocyte colony stimulating factor. They suggest that, rather than the SAA, the water coordination number (WCN) of the Met residues that incorporates both protein and solvent dynamics is a better predictor of the rates of Met oxidation in proteins.

[†] This research was supported by grants from Amgen Inc.

* Corresponding authors. Mailing address: Department of Pharmaceutics, Amgen Inc., One Amgen Center Drive, Thousand Oaks, CA 91320. S.K.: tel, (805)-447-2153; fax, (805)-375-5794; e-mail, skrishna@amgen.com. D.N.B.: tel, (805)-447-8389; fax, (805)-447-3401; e-mail, dbrems@amgen.com.

[‡] University of Colorado Health Sciences Center.

[§] Amgen Inc.

[||] University of Colorado.

[1] Abbreviations: rhIL-1ra, recombinant human interleukin-1 receptor antagonist; CSEP buffer, 10 mM sodium citrate, 140 mM sodium chloride, 0.5 mM EDTA, and 0.1 % polysorbate-20; RP-HPLC, reversed-phase high performance liquid chromatography; CD, circular dichroism; Met or M, methionine; Lys or K, lysine; H_2O_2, hydrogen peroxide.

10.1021/bi700321g CCC: $37.00
Published on Web 05/05/2007

Solution conditions, such as pH (*11*), temperature (*15*), and presence of cosolutes (*5*), can be modulated to reduce Met oxidation by stabilizing the protein's native state. Chemical mutagenesis involving substitution of Met residues by other amino acids is another strategy of preventing protein oxidation and loss of functionality (*16*−*18*). A link between protein's conformational stability and Met oxidation has been shown in a few published studies (*5*). For example, Depaz et al. (*5*) demonstrated that conformational stabilization of subtilisin by the thermodynamic stabilizer sucrose reduced the rate of Met oxidation. Sucrose shifted the protein population toward species with a more compact conformation. As a result, susceptibility of the partially buried Met residue to oxidation and the loss of enzyme activity were reduced.

To gain insights into the nature of the interactions between conformational stability and Met oxidation, we have investigated Met oxidation in recombinant human interleukin-1 receptor antagonist (rhIL-1ra). The overall goal was to document how thermodynamic properties (ΔG_{H2O}, m, and C_m) govern Met oxidation in rhIL-1ra. The understanding derived from such studies is important in developing stabilization strategies against Met oxidation in therapeutic protein formulations and is also crucial in understanding disease conditions where Met oxidation is involved. rhIL-1ra was chosen as the model protein for this study because its crystal structure indicates the presence of Mets with distinct degrees of solvent accessibility (*19*, *20*). There are 6 Met residues in rhIL-1ra; the Mets at positions 11, 126, 137, and 143 have been analyzed in this study (Figure 1). The Met at position 1 has been introduced in the sequence of the recombinant protein for expression purposes in *Escherichia coli* and is not shown in Figure 1. Structurally, this 153 amino acid residue protein exhibits β-trefoil topology with each trefoil consisting of four β-strands and a total of 12 strands.

There are two components to our study. We first examined the conformational stability of rhIL-1ra by performing equilibrium urea unfolding studies over the temperature range 5−50 °C. The temperature dependence of thermodynamic parameters ΔG_{H2O} (free energy of unfolding in the absence of denaturant), m (denaturant concentration dependence of ΔG), and C_m (concentration midpoint for denaturant induced-unfolding) were evaluated. From the temperature dependence of ΔG_{H2O}, the stability curve for the protein was constructed using the Gibbs−Helmholtz relationship (*21*).

Second, we measured H_2O_2 induced oxidation rates of Mets at temperatures between 5 and 45 °C, for buried and surface exposed residues in rhIL-1ra. Monitoring Met oxidation in buried and surface exposed residues allowed us to assess the role of solvent accessibility in correlations between thermodynamic stability and oxidation.

An intrinsic challenge in understanding the effects of protein conformational stability on Met oxidation involves separating conformational dependence from the temperature dependence of reaction kinetics. This was achieved by the analysis of Met oxidation kinetics during coincubation of rhIL-1ra with peptides, which are representative of specific regions of the protein and carry the reactive Met residues. For the analysis of a buried residue, we monitored the rates of oxidation of Met-11 in the protein. rhIL-1ra was coincubated at equimolar concentrations with peptide-1 (SSK**M**-QAFRIWDV), which has the Met corresponding to Met-11 in rhIL-1ra. This strategy allowed us to determine simultaneously the oxidation kinetics of Met-11 in the conformationally constrained protein and in conformationally unconstrained peptide-1 in the same sample.

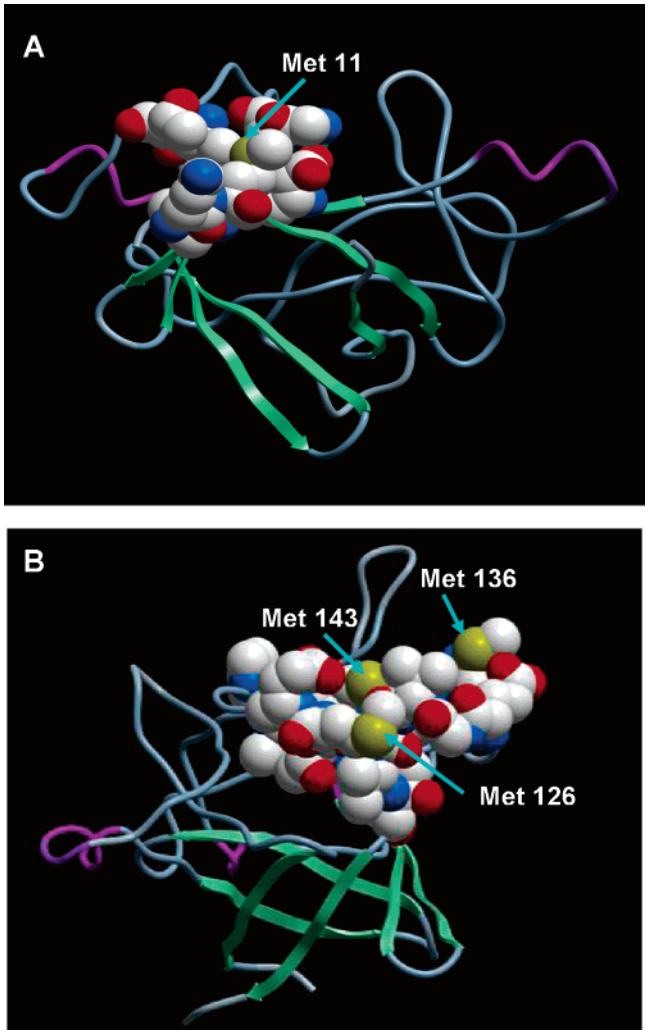

FIGURE 1: Crystal structure of rhIL-1ra (PDB ID: 1ILR) showing (A) Met-11 and (B) Met-126, Met-137, Met-143. The computer graphics and modeling of rhIL-1ra utilized DS Viewer Pro (Accelrys Inc., CA), MOLMOL (*42*), MolSoft ICM browser softwares. Color scheme: helices, dark pink; β-strands, green; β-turns, green; loops, gray. The carbon atoms are shown in white; oxygen, red; nitrogen, blue; sulfur, yellow.

As representative of surface-exposed Met residues, we monitored the rates of oxidation of the three C-terminal Mets in rhIL-1ra, Met-126, Met-137, and Met-143. The analysis of a single peptide from the peptide map containing these three methionines stems from a preliminary investigation that showed first-order kinetics for their oxidation (data not shown). This led to our assumption that their oxidation rates are similar for each Met, and hence the triple Mets were treated as a single entity. For the oxidation of these Mets, rhIL-1ra was coincubated at equimolar concentrations with peptide-2 (TA**M**EADQY) and peptide-3 (TN**M**PDEGV**M**-VTKF). The Met residues in these peptides are representative of Met-126, Met-137, and Met-143 in rhIL-1ra. Again, the Met oxidation kinetics was determined for the peptide and protein in the same sample. In this case, the Mets in the protein are expected to be equally susceptible to oxidation

as the corresponding Met in the peptide. The coincubation technique used in this study has an important advantage over separately incubated samples because the Met residues in both the protein and peptide see identical amounts of reactive, oxidizing species. This is critical since sample-to-sample differences could lead to slight changes in the concentration of oxidizing species and result in significant variations in reaction rates.

MATERIALS AND METHODS

Materials. rhIL-1ra was provided by Amgen Inc. (Thousand Oaks, CA). The purified protein was obtained as a stock solution of 220 mg/mL in pH 6.5 buffer (CSE buffer: 10 mM sodium citrate, 140 mM sodium chloride, 0.5 mM EDTA). The stock protein was dialyzed against excess CSEP buffer, pH 6.5 (CSEP buffer: 10 mM sodium citrate, 140 mM sodium chloride, 0.5 mM EDTA, 0.1% polysorbate 80). High purity urea was purchased from MP Biomedicals (Salon, OH). Ultrapure H_2O_2 was obtained from J. T. Baker (Phillipsburg NJ). Endoproteinase Lys-C (sequencing grade) was purchased from Roche Diagnostics (Indianapolis, IN). Bovine catalase was purchased from Sigma Chemical Company (St. Louis MO). All other chemicals used were of reagent grade or higher. The peptides used in the study were generated and supplied by Amgen Inc. The peptide sequences were the following: peptide-1, SSK**M**QAFRIWDV; peptide-2, TA**M**EADQY; and peptide-3, TN**M**PDEGV**M**VTKF.

Conformational Stability Studies. Urea induced unfolding of rhIL-1ra was monitored in a Jasco circular dichroism spectrometer (model J720) at temperatures of 5, 10, 15, 20, 25, 30, 37, 40, 45, and 50 °C. A urea stock solution (~10.0 M) was prepared in CSEP buffer and pH adjusted to 6.5. The concentration of the urea stock solution was determined by refractive index measurements on a refractometer (Bausch and Lomb) as described by Pace (*22*). Each set of samples were studied isothermally, and fresh samples were prepared and used for each temperature. A stock solution of rhIL-1ra at 22.0 mg/mL was prepared in CSEP buffer to allow for dilution with other components of the solution. The protein concentration for the experiments was determined on an Agilent spectrophotometer (model 8453) using an extinction coefficient of 0.77 (mL^{-1} mg^{-1} cm^{-1}) at 280 nm. rhIL-1ra stock was diluted in CSEP buffer and urea stock solution to the desired final urea concentrations between 0 and 8.0 M and a fixed protein concentration of 1 mg/mL. Samples were incubated at each temperature and in a thermostatted cuvette to ensure equilibrium before measurements were made. At temperatures between 5 and 50 °C, samples were equilibrated overnight at each temperature. Between 30 and 50 °C, samples were initially equilibrated at room temperature and then at the required final temperature for 2 h prior to measurement. Circular dichroism at 230 nm was used to monitor urea induced unfolding of rhIL-1ra between 5 and 50 °C. The mean residue ellipticity at 230 nm for the protein was recorded in a 1.0 mm path length cuvette as an average of a 60 s kinetic scan, with a bandwidth of 2.0 nm and response time of 4.0 s. The reversibility of rhIL-1ra unfolding in urea was tested by recording scans at room temperature and after dilution of samples containing urea to lower subdenaturing urea concentrations. Shock dilution of samples to lower denaturant concentrations resulted in reversibility lower than expected with sequential dilution process. Reversibility was greater than 90% between 5 and 40 °C and above 60% at higher temperatures. A two-state approximation was used to analyze the transition between the native and the denatured states of the protein. The data in the transition region was analyzed using a linear extrapolation model to obtain the thermodynamic parameters: ΔG_{H2O}, m, and C_m (*23*).

Endoproteinase Lys-C Digestion of rhIL-1ra for Analysis of Oxidized Methionines. The analysis of oxidation of specific Met residues in rhIL-1ra required a robust peptide map from which peak areas corresponding to Met containing regions could be isolated and monitored. rhIL-1ra was digested with endoproteinase Lys-C, which cleaves preferentially at the carboxy side of the nine lysine residues of rhIL-1ra producing up to 10 fragments for rhIL-1ra. About 200 μg of rhIL-1ra from samples at 0.5 mg/mL (concentration used in the coincubation study) were dissolved in 150 μL of digestion buffer (50 mM Tris HCl, 0.8 M GdnHCl at pH 8.0). Endoproteinase Lys-C was prepared at a concentration of 0.1 μg/μL in the digestion buffer and added to the protein sample to obtain a final enzyme:substrate ratio of 1:50 by weight. No reduction and alkylation steps were necessary during enzyme digestion since rhIL-1ra does not contain any disulfides. The enzyme treated samples were incubated at 37 °C for 16 ± 1 h to allow for complete digestion of the protein. Enzyme digestion was halted by acidification with 10% TFA, and the digested samples were stored at 4 °C. The fragments generated from Lys-C digestion were analyzed using reversed-phase HPLC and mass spectrometry.

RP-HPLC−Mass Spectrometric Analysis of the Peptide Map. The fragments from Lys-C digestion of rhIL-1ra were separated on a Jupiter C4 column (Phenomenex, 00F-4167-B0) and detected spectroscopically at a wavelength of 215 nm. The mobile phases used were solvent A (0.1% TFA in water) and solvent B (0.1% TFA in 90% acetonitrile). The separation of peptides was performed at 50 °C using a flow rate of 0.2 mL/min with an initial equilibration using 5% solvent B for 3 min, then a ramp to 50% solvent B in 50 min and 90% solvent B in 53 min, and finally 5% solvent B from 54 to 75 min. Masses of the peptides generated were identified by introducing the sample directly from the HPLC column onto a Finnigan LCQ mass spectrometer equipped with an ion-trap mass detector (Thermo Finnigan, San Jose, CA). Mass spectra were collected over the m/z range 400−2300, and the peptide sequence information was obtained from the MS/MS data collected. In an identical procedure, the peptide map and mass spectrometric analysis was carried out on the protein after oxidation with 1 mM H_2O_2 to validate the applicability of the Lys-C digestion method to identify oxidized methionine peaks and mass.

Chemical Stability Studies: Coincubation To Study Oxidation of Protein and Peptide with H_2O_2. Coincubation of rhIL-1ra with Peptide-1. rhIL-1ra (0.5 mg/mL) was coincubated with peptide-1 (SSK**M**QAFRIWDV) at equimolar concentrations (28.9 μM) in CSEP buffer at pH 6.5. Preliminary experiments revealed that protein aggregation could be a competing reaction for oxidation especially at high temperatures and at relatively high protein concentrations. To identify the protein concentration at which aggregation could be diminished during the reaction time for oxidation, aggregation was monitored in CSEP buffer at protein

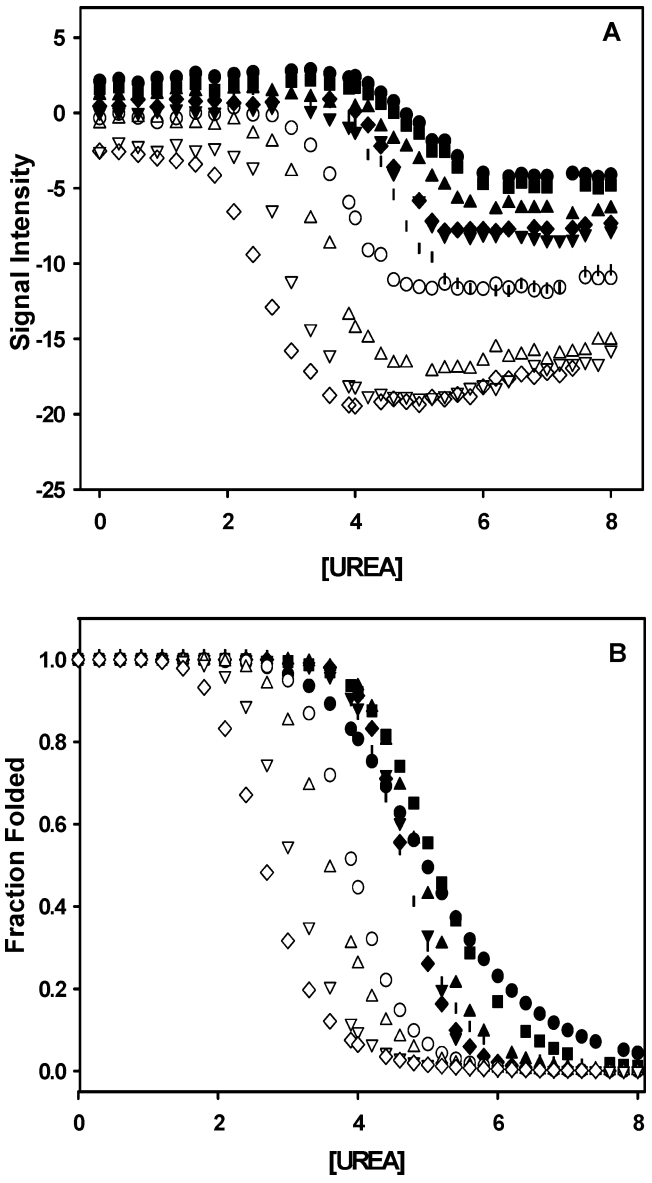

FIGURE 2: (A) Change in circular dichroism at 230 nm for rhIL-1ra at different urea concentrations in CSEP buffer between 5 and 50 °C. (B) Fraction folded plots obtained from the equilibrium urea denaturation curves of panel A ●, 5 °C; ■, 10 °C; ▲, 15 °C; ▼, 20 °C; ◆, 25 °C; |, 30 °C; ○, 37 °C; △, 40 °C; ▽, 45 °C; ◇, 50 °C.

concentrations between 0.5 mg/mL and 2 mg/mL at 45 and 50 °C, because the protein was more susceptible to aggregation at elevated temperatures (*24*). No protein loss due to aggregation was detected at 0.5 mg/mL at these temperatures for up to 10 days (data not shown). Hence, a final rhIL-1ra concentration of 0.5 mg/mL was chosen to perform oxidation experiments.

The oxidation of the protein is not significant in CSEP buffer during storage at 25 °C. As a result, H_2O_2 was added in to the solution to accelerate oxidation. Oxidation was initiated by the addition of H_2O_2 to a final concentration of 1 mM. A 1 mL sample was incubated at each time point in a 1.5 mL eppendorf tube at 5, 15, 25, 30, 37, and 45 °C. At the end of each hour for up to 10 h, oxidation was terminated by the addition of 1.0 μL of bovine catalase to 1.0 mL of sample. The samples were centrifuged at 5000*g* (5 min at 25 °C) and the supernatant was collected. Then the oxidized, coincubated samples were digested with endoproteinase Lys-C and analyzed as described above. A 75.0 μL portion of sample from each time point was injected onto a C4 column, and the extent of oxidation of Met-11 in the protein and in peptide-1 was determined from the peptide map.

Coincubation of rhIL-1ra with Peptide-2 and Peptide-3. In a second set of coincubation experiments, rhIL-1ra (0.5 mg/mL) was incubated with peptide-2 (TA**M**EADQY) and peptide-3 (TN**M**PDEGV**M**VTKF) at equimolar concentrations (28.9 μM of each peptide) and samples were maintained at 5, 15, 25, 30, 37, or 45 °C. Oxidation of coincubated samples with H_2O_2 and protein digestion with endoproteinase Lys-C were carried out as described above. After termination of oxidation with catalase, each oxidized sample was divided into two aliquots. One aliquot was directly injected into the reversed-phase column, and the degree of methionine oxidation in peptides-2 and -3 was determined. The second aliquot was digested with Lys-C and then used for reversed-phase chromatography. Such difference in treatment was necessary since intact peptide peaks coeluted with peptides from Lys-C digestion of the protein. The analysis of oxidation in the C-terminal Mets, that is, Met-126, Met-137, and Met-143, of the protein was carried out by monitoring the peak corresponding to these three Mets from the peptide map.

Kinetic Analysis of Methionine Oxidation in rhIL-1ra and Peptides. Pseudo-first-order rate constants were obtained for the initial rate of Met oxidation, assuming an excess molar concentration of H_2O_2 in the reaction. The decrease in Met containing peptide peak areas with time was monitored. By using the corresponding unincubated peak area at each temperature, the percentage of unoxidized Met was calculated. The percentage unoxidized Met in the protein or peptide was normalized to their initial concentrations, and the rate constants for Met oxidation in protein and peptide were obtained from the slopes of the best-fit lines to the semilog plots of percentage of unoxidized Met versus time.

RESULTS

Equilibrium Denaturation of rhIL-1ra by Urea. The mean residue ellipticity at 230 nm versus urea concentration and the fraction folded plots obtained at different temperatures are shown in Figure 2A and B. rhIL-1ra has a melting temperature (T_m) of 62 °C as measured by a thermal denaturation scan using CD spectral analysis (*24*). However, the onset of thermal denaturation for the protein starts at approximately 55 °C, and unfolding may become irreversible at temperatures above this. At temperatures used in this study, urea denaturation of rhIL-1ra was highly reversible.

The plot of mean residue ellipticity at 230 nm versus urea concentration was sigmoidal. The plot at each temperature was approximated to a two-state transition between the native and unfolded states (*23*). Similar estimates for ΔG_{H2O} were obtained when unfolding of rhIL-1ra was monitored by CD and fluorescence spectroscopies (data not shown). A nonlinear regression of each curve shown in Figure 2A by fitting to eq 1 provided the slope (m_f) and intercept of the upper asymptote (y_f), the slope (m_u) and intercept (y_u) of the lower asymptote, and the slope and inflection point of middle region (C_m).

$$y = \{y_f + m_f[\text{urea}]\} + \{(y_u + m_u[\text{urea}]) \exp[m[\text{urea}]]\} \quad (1)$$

$$\Delta G = -RT \ln K = -RT \ln[(y_f - y)/(y - y_u)] \quad (2)$$

$$\Delta G = \Delta G_{H2O} - m[\text{urea}] \quad (3)$$

Using eqs 1 and 2, ΔG for each denaturant concentration was calculated. From the ΔG values in the transition region (in which there is approximately 20−80% folded protein), the free energy of unfolding in the absence of denaturant (ΔG_{H2O}) and the *m* values were estimated by the linear extrapolation model given by eq 3 (*23*). The *m* value, which is defined as the denaturant concentration dependence of ΔG, reflects the degree of solvent exposure of the hydrophobic groups of the protein in the presence of denaturant (*25*). As seen in Figure 3, the ΔG_{H2O}, *m*, and C_m values exhibited nonlinear temperature dependence. The maximum value of free energy of unfolding was obtained at 25 °C. The change in ΔG_{H2O} as a function of temperature was fitted to the Gibbs−Helmholtz equation (eq 4) to derive the stability curve (Figure 3A) for the protein (*21*):

$$\Delta G_{H2O}(T) = \Delta H(1 - T/T_m) + \Delta C_p(T - T_m - T \ln(T/T_m)) \quad (4)$$

where *T* is the temperature, $\Delta H(T)$, $\Delta S(T)$, and ΔC_p are the changes in the enthalpy, entropy, and heat capacity at each temperature respectively and T_m is the midpoint of unfolding temperature at which the fraction of folded and unfolded protein are equal and thus $\Delta G(T_m) = \Delta H(T_m) - T_m \Delta S(T_m) = 0$. The change in ΔG_{H2O} with temperature was similarly fit to eq 4, with the additional constraint that ΔH be negative to estimate the thermodynamic parameters for the low temperature side of the stability curve (*26*). The calculated values are shown in Table 1.

Lys-C Peptide Map for rhIL-1ra To Monitor Methionine Oxidation Rates. Figure 4A and B illustrates the reversed-phase HPLC separation of peptides from endoproteinase Lys-C digestion of unoxidized and oxidized rhIL-1ra respectively. The Lys-C digestion protocol was optimized to ensure that there was no intact rhIL-1ra remaining after digestion. Intact rhIL-1ra eluted at ∼42 min. After Lys-C digestion, only negligible amounts of intact rhIL-1ra remained. Presence of large or variable amounts of intact protein after the digestion step can result in inaccurate estimates of oxidation rate constants as observed from the loss of Met containing peptides. The nine peptides from Lys-C digestion are numbered sequentially starting from the N-terminus of the protein as K1 through K9. All peptides from Lys-C digestion of rhIL-1ra were recovered except K2, which was too hydrophilic to be retained on the reversed-phase column. The sequence of the different fragments generated and their corresponding masses are shown in Table 2.

A comparison of Lys-C peptide map of the oxidized and native protein reveals no change in the chromatogram apart from a shift to lower retention times for Met oxidized peaks and a concomitant increase in mass corresponding to the addition of an oxygen atom. The addition of an oxygen atom to the Met to form MetSO increased the polarity of the

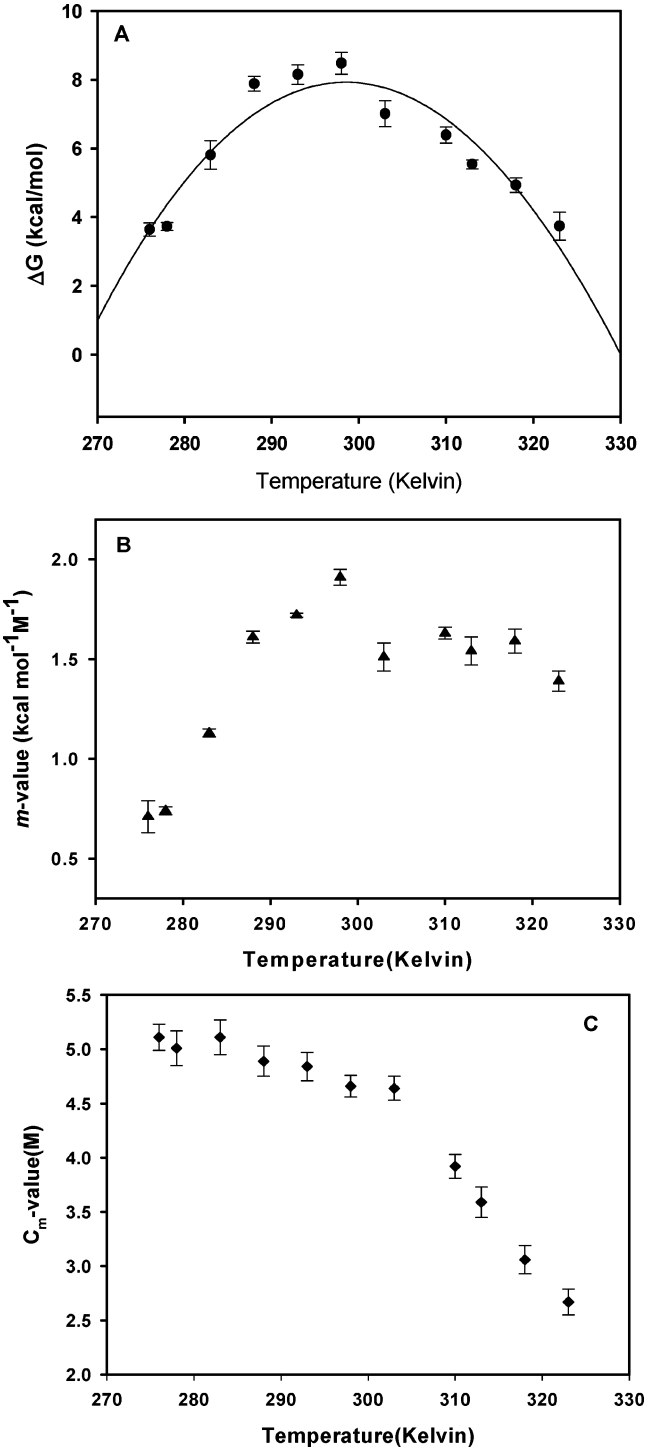

FIGURE 3: Temperature dependence of (A) ΔG, (B) *m*, and (C) C_m values for rhIL-1ra from urea unfolding studies under isothermal conditions between 5 and 50 °C. Solid line in panel A was the best fit to eq 4 to the plot of ΔG vs temperature. ΔG values reflect ΔG_{H2O} obtained in the absence of denaturant. The error bars in all panels were calculated from duplicate sets of samples.

peptide, which resulted in earlier elution from the reversed-phase chromatography (*4*). The prepeak that eluted before peptide K3 labeled K3A (Figure 4A and 4B) showed an increased mass of 16.1 Da suggesting oxidation of Met-11 in this fragment. The oxidation of the C-terminal peptide K9 resulted in K9A (Figure 4A and 4B), with a mass increment of 48.3 Da suggesting oxidation of all three Mets in this region. The oxidized form of K9, K9A, appears in the peptide map as a split peak. The K9A is a split peak

Table 1: Thermodynamic Parameters Obtained from the Stability Curve of rhIL-1ra[a]

	ΔH (kcal/mol)	ΔC_p (kcal mol^{-1} K^{-1})	T_m (K)
heat denaturation	163.44 ± 1.27	4.94 ± 0.04	329.90 ± 0.28
cold denaturation	−142.31 ± 1.11	4.94 ± 0.04	268.09 ± 0.43

[a] The mean ± SD were calculated from duplicate set of samples.

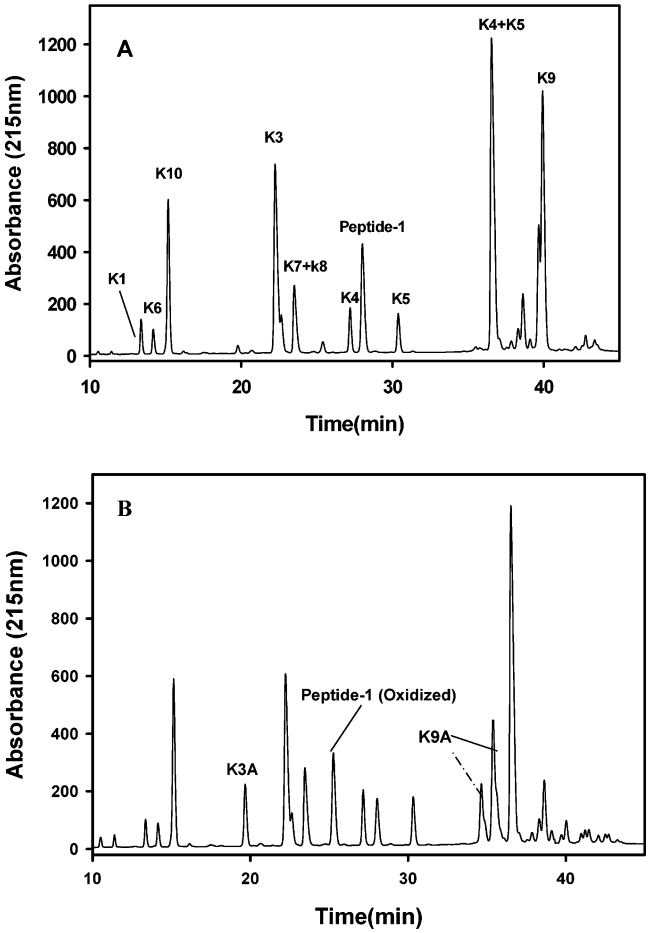

FIGURE 4: (A) Reversed-phase chromatogram showing the Lys-C peptide map for rhIL-1ra during coincubation with peptide-1 and after hydrogen peroxide treatment for 1 h at 25 °C. (B) The formation of methionine oxidized peptide peak for Met-11 (K3A) in rhIL-1ra and peptide-1 is shown along with the oxidized peak for C-terminal methionines (K9A). The oxidized peaks are indicated with a suffix A to the main peak.

because oxidation of Met to MetSO forms a new chiral center at sulfur atom and results in a racemic mixture of diastereomeric peptides (*27*). Both peaks within the "doublet" showed a mass increment corresponding to oxidation of the three methionines. However, the diastereomeric peptide sulfoxides may be resolved by RP-HPLC only in certain cases with Met forming MetSO. Other Met containing peptides K1 (Met-1) and K6 (Met-66) were also identified from the peptide map and mass spectral analysis but not monitored for their oxidation kinetics. The peptide sequence with Met 66 contains the two cysteine residues (YGIHGGKMCLSCVKSG). Our preliminary experiments indicated that the free cysteines in the peptide cross-link with the protein and between themselves on coincubation thus complicating analysis.

Oxidation of Met-11, Met-126, Met-137, and Met-143 in rhIL-1ra and Peptides. The rate of disappearance of peak K3 was monitored to estimate the extent of oxidation of Met-11 in rhIL-1ra (Figure 4A). The intrinsic oxidation rate of Met-11 was determined in peptide-1 (SSK**M**QAFRIWDV) from the peptide map after proteolytic treatment of the coincubation sample (Figure 4B). The Lys-C proteolytic cleavage of peptide-1 at its lysine residue gave rise to smaller peptides SSK and **M**QAFRIWDV. The peptide SSK was not retained during reversed-phase chromatography, however both oxidized and unoxidized peaks corresponding to **M**QAFRIWDV were well resolved from the other peaks in the peptide map. The time course of the change in concentration of unoxidized Met and the pseudo-first-order rate constants calculated for Met-11 oxidation in rhIL-1ra and peptide-1 are shown in Figure 5A and B and Table 3 respectively. The linearity of the plots is consistent with that expected for pseudo-first-order oxidation reactions.

The oxidation rates of Met-11 in both protein and peptide-1 increased with temperature, although at any temperature the rate was significantly higher in the peptide (Table 3). H_2O_2 has been shown to react faster toward surface exposed Met residues compared to buried residues of the protein (*11*). Thus, the differential reactivity of Met-11 in protein versus peptide to the oxidizing species provides some insight to their relative degrees of protection. The faster rate of oxidation for the Met-11 in peptide-1 was due to the lack of conformational constraints compared to the slower oxidation of the same Met in the protein and suggests protection of this residue in rhIL-1ra. The crystal structure of rhIL-1ra indicates that Met-11 is positioned on a β-strand in the protein with its sulfur atom being oriented toward a cleft surrounded by amino acids glycine-10, aspartic acid-47, valine-50, glycine-63, glycine-64, iso-leucine-86, and threonine-87, limiting its accessibility to the oxidizing species in solution. The solvent accessibility of the sulfur atom in Met-11 (Figure 1A), to which the oxygen atom attaches during oxidation, was calculated to be 9% in rhIL-1ra (MOLMOL). The Met-11 oxidation rates in the protein were slower than in peptide-1 at all temperatures and are reflected by ratios of (oxidation rate of Met-11 in protein)/(oxidation rate of Met-11 in peptide) in Table 3. The increased ratio of oxidation of Met-11 in (protein/peptide) with temperature suggests decreased protection provided by the conformation of the protein with increased temperature.

The change in peak area for peptide K9 shown in Figure 4A was followed to determine the extent of oxidation of Met-126, Met-137, and Met-143 in the protein. As indicated in the Materials and Methods section, the analysis of intrinsic rates of oxidation in Met-126, Met-137, and Met-143 in peptides-2 and -3 that were coincubated with the protein was carried out by directly injecting the coincubation mixture onto the reversed-phase chromatography. Figure 6 illustrates chromatograms that show the C-terminal Met oxidation in peptides-2 and -3 obtained from intact coincubation sample injection. Figure 7 shows the time course of oxidation of Met-126, Met-137, and Met-143 in the protein and peptide. The calculated pseudo-first-order rate constants for their oxidation are shown in Table 4. The rate constants for the three Mets in rhIL-1ra and the peptide increased with temperature. Interestingly, the rate constant for the three-Met oxidation in rhIL-1ra was similar to that of the peptide

Table 2: Endoproteinase Lys-C Digested Peptides of rhIL-1ra Shown in Figure 4A and 4B

peptide	residue no.	obsd sequences of rhIL-1ra from Lys-C digestion	mass obsd	mass obsd with methionine oxidation
K1	1−7	**M**RPSGRK[a]	831.01	846.81 (+15.8)
K2	8−10	SSK[b]	320.35	
K3	11−22	**M**QAFRIWDVNQK[a]	1535.78	1551.88 (+ 16.1)
K4	23−46	TFYLRNNQLVAGYLQGPNVNLEEK	2781.11	
K5	47−65	IDVVPIEPHALFLYGIHGGK	2012.38	
K4 + K5	23−65	TFYLRNNQLVAGYLQGPNVNLEEK IDVVPIEPHAL FLYGIHGGK[c]		
K6	66−72	**M**CLSCVK[a]	783.04	799.14 (+ 16.1)
K7	73−94	SGDETRLQLEAVNITDLSENRK	2488.69	
K8	95−97	QDK	389.41	
K9	98−146	RFAFIRSDSGPTTSFESAACPGWFLCTA**M**EADQPV SLTN**M**PDEGV**M**VTK[a]	5301.00	5349.3 (+48.3)
K10	147−153	FYFQEDE	976.99	

[a] All oxidizable methionines have been highlighted in the sequence. [b] Peptide K2 is hydrophilic and not retained in the reversed-phase column. [c] Peptide K4 + K5 was generated from a miscleavage at residue K-46.

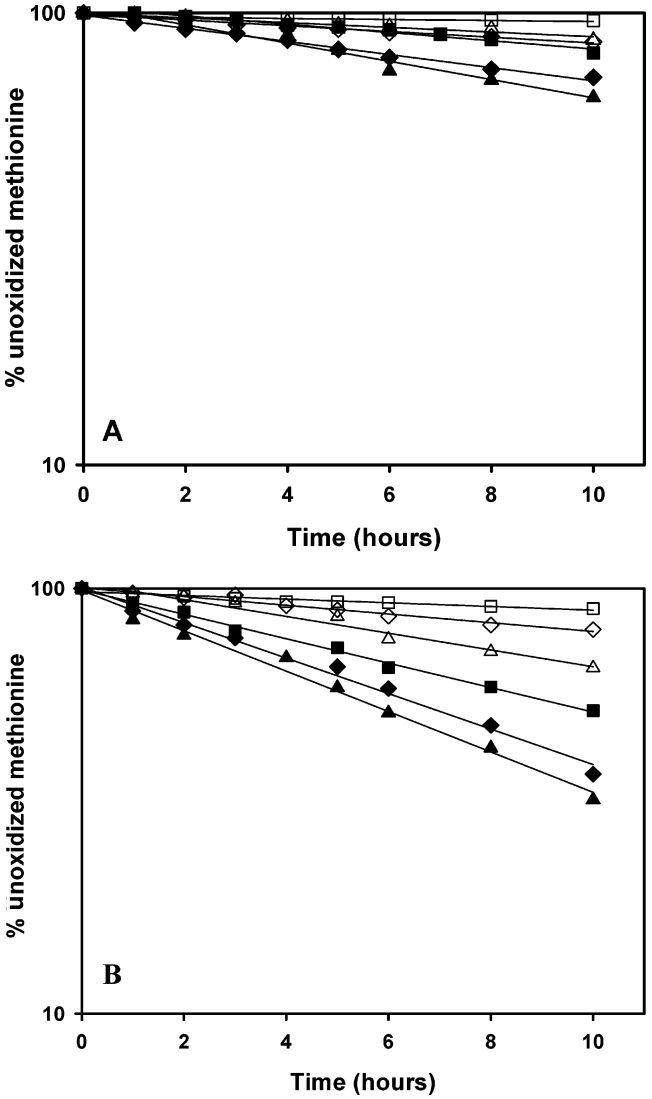

FIGURE 5: Time course of change in oxidation of methionine (Met-11) in (A) rhIL-1ra and (B) peptide-1. Oxidation was with 1 mM H_2O_2 in CSEP buffer (pH 6.5) between 5 and 45 °C: □, 5 °C; ◇, 15 °C; △, 25 °C; ■, 30 °C; ◆, 37 °C; ▲, 45 °C.

at all temperatures. This is presumably due to the similar extent of solvent exposure of the C-terminal Mets in rhIL-1ra as for the Mets in the peptides-2 and -3. In other words, there is an absence of conformational protection for these C-terminal Mets. The sulfur atoms in the three C-terminal

Table 3: Pseudo-First-Order Rate Constants for the Oxidation of Met-11 in rhIL-1ra and the Corresponding Methionine in Peptide-1[a]

temp (°C)	Met-11 in rhIL-1ra (h^{-1})	Met-11 in peptide-1 (h^{-1})	*k* oxidation protein/ *k* oxidation peptide[b]
5	0.002 ± 0.0003	0.012 ± 0.0008	0.149 ± 0.012
15	0.006 ± 0.0003	0.029 ± 0.0014	0.187 ± 0.019
25	0.008 ± 0.0004	0.045 ± 0.0024	0.203 ± 0.002
30	0.015 ± 0.0002	0.054 ± 0.0009	0.213 ± 0.006
37	0.023 ± 0.0016	0.090 ± 0.0016	0.253 ± 0.014
45	0.037 ± 0.0020	0.133 ± 0.0033	0.282 ± 0.008

[a] The mean ± SD were calculated from duplicate set of samples. [b] From each set of the replicate, the ratio of protein/peptide oxidation rate was calculated. For duplicate samples at a given temperature, an average and SD were calculated as shown in column 4.

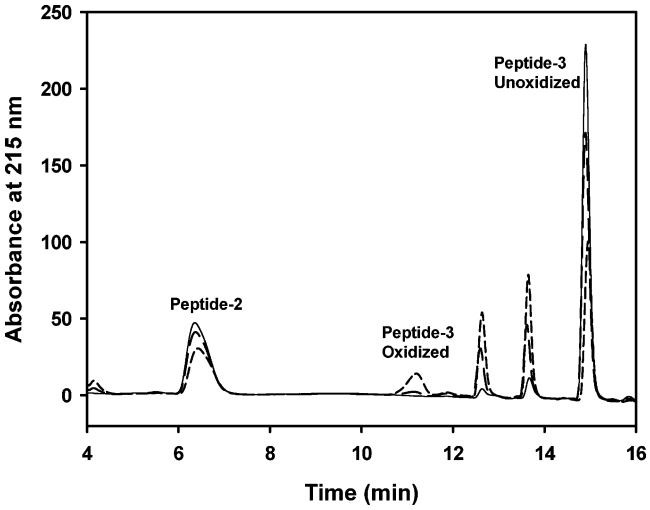

FIGURE 6: Reversed-phase chromatograms of intact rhIL-1ra coincubated at 25 °C with peptide-2 and peptide-3. Intact coincubated samples (undigested) were injected and peak areas corresponding to peptides-2 and -3 were used in the analysis of oxidation in these peptides. Descending peak areas of unoxidized peptide-2 and peptide-3 shown above indicate the progress of oxidation after 0, 4, and 8 h.

Mets are highly solvent accessible (Figure 1B). The solvent accessibility of the sulfur atoms in the methionines was calculated to be 90%, 78%, and 49% for Met-126, Met-137, and Met-143 respectively. We consistently observed at all temperatures a slightly greater rate of oxidation of C-terminal Mets in the protein relative to the peptide (Table 4). However, the observed differences in the rates at any given

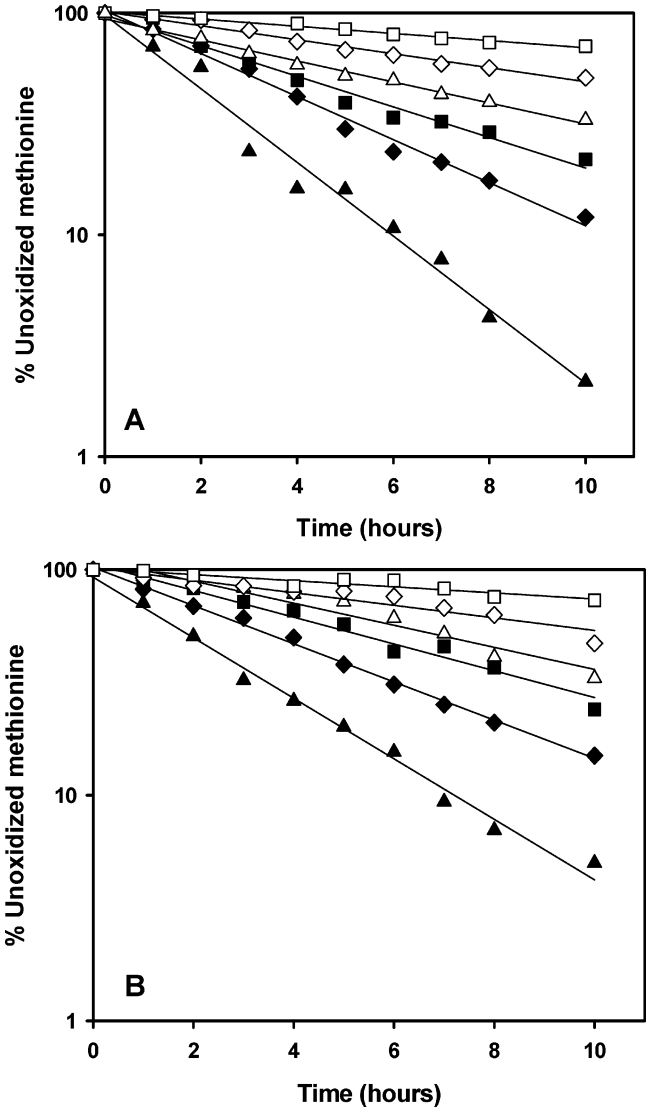

FIGURE 7: Time course of change in oxidation of C-terminal methionines (Mets-126, -137, -143) in (A) rhIL-1ra and (B) peptides-2 and -3. Oxidation was with 1 mM H_2O_2 in CSEP buffer (pH 6.5) between 5 and 45 °C: □, 5 °C; ◇, 15 °C; △, 25 °C; ■, 30 °C; ◆, 37 °C; ▲, 45 °C.

Table 4: Pseudo-First-Order Rate Constants for the Oxidation of Mets-126, -137, and -143 in rhIL-1ra and the Corresponding Methionine in Peptides-2 and -3[a]

temp (°C)	Met-126, -137, and -143 in rhIL-1ra (h^{-1})	Met-126, -137, -143 peptides (h^{-1})	*k* oxidation protein/ *k* oxidation peptide[b]
5	0.031 ± 0.002	0.022 ± 0.002	1.39 ± 0.14
15	0.051 ± 0.003	0.039 ± 0.002	1.32 ± 0.15
25	0.111 ± 0.008	0.089 ± 0.011	1.26 ± 0.11
30	0.135 ± 0.008	0.106 ± 0.011	1.28 ± 0.11
37	0.164 ± 0.004	0.127 ± 0.009	1.28 ± 0.05
45	0.233 ± 0.017	0.198 ± 0.007	1.25 ± 0.13

[a] The mean ± SD were calculated from duplicate set of samples. [b] From each set of replicate, the ratio of protein/peptide oxidation rate was calculated. For duplicate samples at a given temperature, an average and SD were calculated (column 4).

temperature were not statistically significant ($p > 0.05$ at 95% confidence interval).

The crystal structure of rhIL-1ra illustrates the relative positions of the three C-terminal Mets (Figure 1). Met-126 is positioned in a β-turn region of the protein while Met-137 and Met-143 are both in the loop regions of rhIL-1ra. A preliminary investigation of the oxidation rate of the C-terminal Mets in rhIL-1ra demonstrated a first-order reaction suggesting that the oxidation of these Met residues proceeded independently of each other albeit at a similar rate. This understanding led us to consider the oxidation of the three C-terminal Mets as a group. The oxidation of any single C-terminal Met, Met-126, Met-137, or Met-143, led to loss of peak K9 and contributed to the oxidation rate.

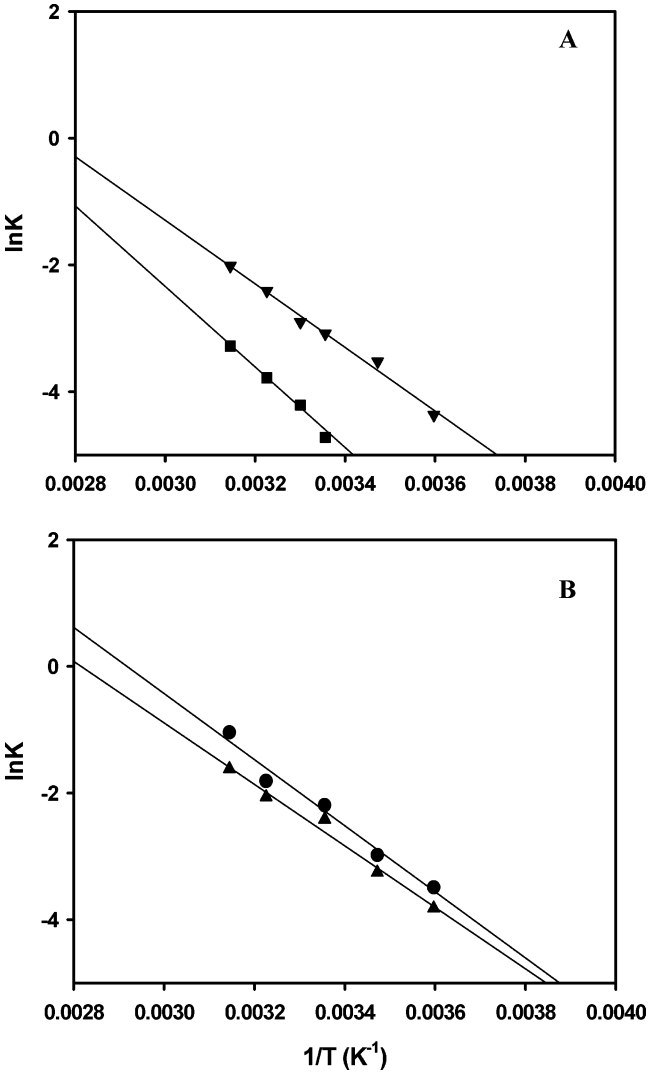

FIGURE 8: Arrhenius plots for determination of the activation energy for oxidation of (A) ■, Met-11 in protein; ▼, Met-11 in peptide-1; (B) ●, Mets-126, -137, and -143 in protein; ▲, Mets-126, -137, and -143 in peptides-2 and -3. The apparent activation energies for oxidation of Met-11 in rhIL-1ra and peptide were 13.2 ± 0.37 kcal/mol and 9.9 ± 0.16 kcal/mol respectively. The activation energies calculated for the oxidation of Mets-126, -137, and -143 in rhIL-1ra and peptide were 9.16 ± 0.40 kcal/mol and 9.74 ± 0.32 kcal/mol respectively.

An Arrhenius plot was constructured from the oxidation rates of the Mets in protein and peptides at different temperatures (Figure 8A and B). The apparent activation energy for oxidation of Met-11 in rhIL-1ra was 13.2 ± 0.37 kcal/mol, which is about 3.2 kcal/mol higher than for the same Met oxidation in peptide. The observed difference in activation energy for oxidation of Met-11 between the protein and peptide was statistically significant (using $p < 0.05$ and 95% confidence interval to indicate statistical significance).

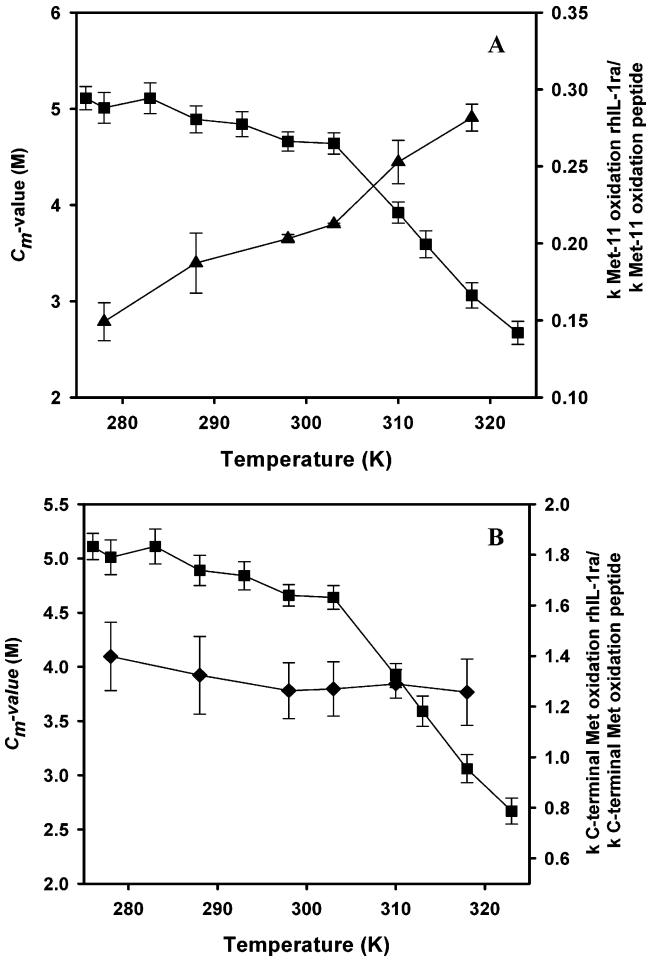

FIGURE 9: Correlation of conformational stability and methionine oxidation: ■, C_m values; (A) ▲, normalized rates for Met-11 oxidation; (B) ◆, normalized rates for Met-126, Met-137, Met-143 oxidation. The normalized rates were calculated from the ratio of oxidation rates of methionine in protein and their rates in the corresponding peptide.

The apparent activation energy for oxidation of Met-126, Met-137, and Met-143 in the protein and peptide were in the same range (9.16 ± 0.40 kcal/mol vs 9.74 ± 0.32 kcal/mol), and any difference between them was statistically insignificant ($p > 0.05$). The rate constants for the buried and exposed Met oxidation in the protein were normalized to the rate of Met oxidation in the corresponding peptide to assess the degree of protection by protein conformation. The normalized rates were correlated to the thermodynamic parameters from equilibrium unfolding (Figure 9).

DISCUSSION

Thermodynamic Stability of rhIL-1ra. The conformation of the native protein (i.e., in the absence of urea) only varied slightly with temperature (Figure 2A). In contrast, the raw CD signal for rhIL-1ra versus urea concentration showed different post-transition plateaus at the different temperatures studied (Figure 2A). This result suggests that the unfolded states of the protein differ as a function of temperature. Because it is possible to go from one type of unfolded state to another in a cooperative process with no change in thermodynamic properties, these states were treated as being thermodynamically indistinguishable (*28*). Thus the transitions at each temperature were approximated by a two-state process to generate the fraction folded plots.

From the equilibrium denaturation of rhIL-1ra by urea, the thermodynamic parameters of ΔG_{H2O}, m, and C_m were estimated. The free energy of unfolding (ΔG_{H2O}) of the protein decreased on either side of the optimum temperature for maximum stability and provided the complete free energy profile for rhIL-1ra. The ΔG_{H2O} values for the protein from urea unfolding were in good agreement with the free energy values estimated previously for rhIL-1ra at 37 °C from urea induced unfolding studies (*29*). The ΔG_{H2O} dependence on temperature derives contributions from the change in m and C_m values with temperature. The m and C_m values for rhIL-1ra showed nonlinear temperature dependency: the m value increased with temperature, and the C_m values decreased with increased temperature. Different trends of temperature dependencies have been noted for these parameters by previous investigators. The m value has been typically correlated to the amount of protein surface area exposed upon unfolding in the presence of a denaturant (*25*). In some of the earlier studies on small globular proteins like barstar, ferric uptake regulator (Fur A), histidine containing phosphocarrier protein (*E. coli* HPr), and muscle acylphosphatase, it has been reported that the m value is independent of temperature (*26*, *30*−*32*). More recently for globular proteins, histidine containing phospho carrier protein from *Streptomyces coelicolor* (*33*), and hisactophilin (*34*), linear temperature dependence has been observed where the m value decreased with increased temperature. These workers suggested that this temperature dependent decrease may be larger for larger proteins. The m value for maltose binding protein (MBP), a large monomeric two-domain protein containing 370 amino acids, was strongly temperature dependent, and the values decreased on either side of the stability maximum (*35*). In contrast to the observations made with other proteins, the m value for rhIL-1ra increased significantly between 5 and 25 °C followed by a gradual decrease or plateau between 30 and 50 °C. This suggested that, for rhIL-1ra, the decreased m value at lower temperatures has a greater contribution to the decreased ΔG_{H2O} at lower temperatures than the C_m values.

The temperature dependent m values in rhIL-1ra could be due to the interplay of several factors. First, the strength of denaturant−protein interactions is weakened at high temperatures (*36*). Zweifel and Barrick (*37*) propose a contribution from the heat capacity change as a result of denaturant−protein interaction. Depending on whether the heat capacity change from urea−protein interaction is positive, negative, or zero, the m value may increase, decrease, or plateau respectively. A negative heat capacity from the urea−protein interaction could lead to decreased m values at lower temperatures as noticed with rhIL-1ra. Since the heat capacity change from the urea−protein interaction has not been examined in this study, we could not assess the contribution from this factor to m value changes. Another possibility could be the structural fluctuations in the protein at varying temperatures. Native rhIL-1ra has been reported to show temperature dependent tertiary structural changes (*38*). Consequently, the overall change in surface exposure upon contact with denaturant solution may be affected by the structural changes in the protein as a function of temperature. The presence of residual structure in the unfolded state at

low temperatures could also affect the extent of exposure of hydrophobic surface area as a result of unfolding and cause the decreased *m* values (*25*). Finally, the origin of a decrease in *m* value has also been attributed to the presence of equilibrium intermediates (*39*). This is unlikely the case because a two-state model adequately describes the unfolding data at each temperature.

Myers et al. (*25*) have shown a strong dependence for *m* value and ΔC_p to the amount of protein surface exposed to solvent upon unfolding and have documented a good correlation between these parameters. The *m* values calculated from urea unfolding of rhIL-1ra are comparable to the values observed for other globular proteins of similar size (*25*). However, the ΔC_p value for rhIL-1ra is much higher than what is observed for other proteins of similar size (Table 1). The heat capacity for unfolding (ΔC_p) of rhIL-1ra was estimated to be 4.94 ± 0.04 kcal mol^{-1} K^{-1} from the stability curve. This value is unusually high for rhIL-1ra compared to the ΔC_p estimate based on 12−16 cal deg^{-1} mol^{-1}/residue, which should result in ~1.9 kcal deg^{-1} mol^{-1}. However the identical values of ΔC_p obtained from analysis of the cold and heat denaturation segments of the stability curve are consistent with the inherent assumption of a temperature independent heat capacity change (*28*). Both these parameters (m, ΔC_p) correlate to changes in solvent accessible area upon unfolding, but different factors contribute to the change in surface area in each case (*32*). ΔC_p value is defined by the curvature of the stability curve. Our interpretation of the large value of ΔC_p is associated with the moderately high ΔG_{H2O} (~8.48 kcal/mol) coupled to the high cold and low heat denaturation temperature for rhIL-1ra. This results in a steep stability curve for the protein where ΔG_{H2O} depends more sharply on temperature.

The C_m values for rhIL-1ra decreased as temperature was increased. Interestingly, rhIL-1ra is more prone to urea induced denaturation at 50 °C relative to 5 °C as indicated by the substantially lower C_m value, while their unfolding free energies are the same at both temperatures. This could be attributed to the difference in end states being populated. Previous investigators have noted both linear (decreased with increased temperature) and nonlinear temperature dependencies of C_m values (*26*, *30*−*35*). For rhIL-1ra, the C_m value showed a temperature dependence opposite in trend to that noted for the *m* value. The C_m value plateaued between 3 and 25 °C and decreased significantly between 30 and 50 °C. The C_m value decreased by 10% from its maximum value at 3 °C relative to 25 °C, while it changed by almost 40% in the temperature range of 30−50 °C. The C_m value directly reflects the conformational stability of the protein at a given temperature and the consequent change in resistance of the protein to denaturant induced unfolding. The significant change in C_m value from 30 to 50 °C is likely due to the decreased conformational stability of the protein over this temperature range.

Methionine Oxidation in rhIL-1ra. The oxidation rates of the Met-11, Met-126, Met-137, and Met-143 in rhIL-1ra showed a strong dependence on temperature and on their relative solvent accessibility. Oxidation of Met-11 in rhIL-1ra proceeded at rates 3 to 7 times slower (depending on temperature) than the observed rates in the corresponding peptide. This suggests that Met-11 is at least partially protected by protein conformation. The Met-11 oxidation rates in rhIL-1ra increased progressively with temperature compared to peptide-1, suggesting possible local conformational changes around the Met residue that increased its susceptibility to oxidation. On the other hand, the oxidation of Met-126, Met-137, and Met-143 in rhIL-1ra proceeded at rates comparable to its rates of oxidation in the peptide at all temperatures. This is presumably due to the similar degrees of solvent exposure of these Mets in the protein and peptide. They oxidized to the same extent as the methionines in the peptide, which are completely exposed to the solvent, indicating that the C-terminal Mets in the protein have no conformational constraints unlike Met-11 in the protein.

Further calculations were made to determine the rate-limiting step of the oxidation reaction. In a reaction such as methionine oxidation, for the Mets in the protein or peptide to be oxidized, the oxidizing species and the protein or peptide must approach each other in solution by diffusion, followed by subsequent binding of the oxygen molecule to the sulfur residue, implicating a possible diffusional limitation mechanism in the reaction kinetics. The role of solvent accessibility of the Mets and water coordination also needs to be considered, as does the size difference between the peptide and protein. The peptide is less structured, smaller, and more solvent exposed than the intact protein, and it has the ability to diffuse faster in solution and may thus be inherently more reactive. Whether the increased diffusion of the peptide due to its smaller size leads to greater reactivity would depend on whether oxidation was diffusion limited. To explore this question, the contribution of a possible diffusion related mechanism in the oxidation of the Mets in the protein or peptide may be assessed by estimating the rate constant (k_d) for the diffusion controlled oxidation reaction between protein-O_2 and peptide-O_2 (eq 5). The diffusivities were calculated for rhIL-1ra and peptide, assuming that both are spheres of radius 2.0 and 1.0 nm respectively. The diffusion limited rate constant was calculated from the Stokes−Einstein equation given below:

$$k_d = 4\pi(D_{O2} + D_{protein})(R_{O2} + R_{protein})N_A \qquad (5)$$

D_{O2} and $D_{protein}$ are the diffusivities of the oxygen and protein (or peptide); R_{O2} and $R_{protein}$ are the radius of the oxygen and protein (or peptide). To obtain the pseudo-first-order rate constant, eq 5 was multiplied by the concentration of H_2O_2 (1 mM), which is assumed to be roughly constant because it is in excess with respect to protein or peptide concentration (*5*). Applying eq 5 resulted in k_d values in the order of 10^7 h^{-1} for the peptide and rhIL-1ra. This is several orders of magnitude larger than the rate constants obtained in Tables 2 and 3. This suggests that the oxidation in neither protein nor peptide is externally diffusion limited. Furthermore, the activation energies calculated for the Met oxidation in protein and peptide were much higher than for a diffusion-limited reaction, which typically have small activation energies on the order of 0.5−1.0 kcal/mol. The activation energies associated with oxidation of Mets in the peptides and Met-126, Met-137, and Met-143 in rhIL-1ra are within the same range (9.0−10 kcal/mol) due to their similar degrees of solvent accessibility. The activation energy for oxidation of Met-11 in the protein was about 3 kcal/mol more than the activation energy associated with Met oxidation in the corresponding peptide. This reiterates that the oxidation of Met-11 in the protein is restricted by its conformation.

Conformational Dependence of Methionine Oxidation in rhIL-1ra. Although protein oxidation has long been linked to conformation, studies investigating the critical thermodynamic property modulating reactivity are limited (*5*). In addition, oxidation reactivity of specific residues is not completely understood. Our goal was to determine relevant thermodynamic parameters modulating Met oxidation in rhIL-ra by investigating for linkages between the conformational stability of the protein and its oxidation. An integral part of the study was to understand the temperature dependence of the thermodynamic parameters ΔG_{H2O}, m, and C_m and the reaction rates for Met oxidation. Figure 9 shows the normalized rates for oxidation of Met-11 and Met-126, Met-137, and Met-143. Comparison of these rates to the results from Figure 3 provides some interesting insights. As expected, the oxidation rate constants of Met-126, Met-137, and Met-143 oxidation showed no correlation to the thermodynamic parameters from equilibrium unfolding and are consistent with the absence of conformational constraints for their oxidation.

Urea induced unfolding studies of rhIL-1ra indicate that rhIL-1ra unfolds through a two state F ↔ U mechanism. The protein is predominantly in the folded state at all temperatures between 5 and 50 °C in the absence of denaturant (Figure 2). This indicates that the oxidation of solvent exposed methionines proceeds even when a large population of protein molecules is in the folded state and matches the extent of oxidation in peptides across the broad range of temperature studied. However, the buried Met-11 oxidation would occur from the unfolded state of the protein. Even at 25 °C, where the thermodynamic stability (ΔG_{H2O}) of rhIL-1ra is maximum, there appears to be a population of unfolded species (which is only a small fraction of the total protein molecules) reactive to Met-11 oxidation. At temperatures higher than 25 °C, unfolding free energies decreased significantly between 30 and 50 °C and were correlated to the increased oxidation rate for Met-11 in this temperature range. The decreases in free energies suggest an increased population of unfolded species. Our calculations based on the free energy values obtained in the absence of denaturant indicate that the percentage of unfolded species may only be 0.002% at 25 °C, while it increases to almost 0.09% at 37 °C and up to ~7.0% at 50 °C (data not shown). This increase coupled to the effect of temperature on reaction rates resulted in the increased oxidation rate of Met-11 between 30 and 50 °C. At temperatures below 25 °C, ΔG_{H2O} for rhIL-1ra decreased to an extent similar to that in the high temperature range. However, even at 5 °C where the ΔG_{H2O} for the protein was a minimum, Met-11 oxidation showed no substantial increase. According to expectations, the decreased ΔG_{H2O} and the resulting increased population of unfolded molecules should lead to increased Met-11 oxidation rate. This lack of correlation is suggested to be due to temperature effect on reaction rates that may suppress the extent of Met-11 oxidation at these low temperatures. Thus, despite the decreased free energies of unfolding at low temperatures (<25 °C), Met-11 oxidation rate was not increased to the same extent as seen at temperatures above 30 °C. This has interesting relevance to accelerated stability testing of protein pharmaceuticals, where usually sample stability at low temperatures for long-term storage is predicted from accelerated storage at high temperatures. Such predictions could result in overestimation of rates and stability values not indicative of the actual stability at the intended temperature of storage.

The m values from equilibrium unfolding experiments showed no correlation to the Met-11 oxidation rates. The biphasic trend of the C_m value as a function of temperature showed good correlation to the Met-11 oxidation rate constants. Between the temperatures 5 and 30 °C, the C_m value for rhIL-1ra slightly decreased and Met-11 rate constants increased. Above 30 °C, the C_m values decreased further rapidly and correlated with the increased Met-11 oxidation rate constants in rhIL-1ra. As the protein became more prone to denaturation (decreasing C_m value), the oxidation rate of Met-11 was increased. The decreased resistance of the protein to the denaturant is a direct consequence of the reduced conformational stability of the native state at that temperature. The correspondence between the C_m value and the intrinsic oxidation rate of Met-11 suggests that thermodynamic stability indicated by C_m value is more relevant to the rate of oxidation of the buried Met in rhIL-1ra. The C_m value has been used by others to define the thermodynamic stability of proteins (*40*, *41*). The buried Met residue oxidation is most affected by the structural and functional destabilization of protein molecules. Understanding how thermodynamic stability correlates to a buried Met oxidation in a protein has implications in the design of accelerated stability studies as well as in predicting the impact of temperature deviations during manufacturing, shipping, and storage of therapeutic protein formulations. Furthermore, such studies are also relevant to disease conditions where Met oxidation has been implicated. Our studies indicate that thermodynamic stability plays an important role in predicting oxidation kinetics for buried methionines in proteins.

ACKNOWLEDGMENT

We are thankful to Ted Bures, Dr. Ramil Latypov, and Dr. Andrei Raibekas for their helpful discussions on the project. We also thank Kevin O'Connor for performing initial development work for this project. Our thanks to Dr. Stephen Brych, Rikki Stevenson, and Dr. Dean Liu for their help in providing the crystal structure and solvent accessible area of methionines in rhIL-1ra. We thank the Apollo peptide synthesis group, Colorado, for their help with synthesizing the peptides for the study.

REFERENCES

1. Meyer, J. D., Ho, B., and Manning, M. C. (2002) Effects of conformation in the chemical stability of pharmaceutically relevant polypeptides, in *Rational Design of Stable Protein Formulations* (Carpenter, J. F., and Manning, M. C., Eds.) pp 85−108, Kluwer Academic/Plenum Publishers, New York.
2. Ferrington, D. A., Sun, H., Murray, K. K., Costa, J., Williams, T. D., Bigelow, D. J., and Squier, T. C. (2001) Selective degradation of oxidized calmodulin by the 20 S proteasome, *J. Biol. Chem. 276*, 937−943.
3. Matheson, N. R., Wong, P. S., and Travis, J. (1979) Enzymatic inactivation of human alpha-1-proteinase inhibitor by neutrophil myeloperoxidase, *Biochem. Biophys. Res. Commun. 88*, 402−409.
4. Teh, L. C., Murphy, L. J., Huq, N. L., Surus, A. S., Friesen, H. G, Lazarus, L., and Chapman G. E. (1987) Methionine oxidation in human growth hormone and human chorionic somatomammotropin- effects on receptor binding and biological activities, *J. Biol. Chem.* **262**, 6472−6477.
5. Depaz, R. A., Barnett, C. C., Dale, D. A., Carpenter, J. F., Gaertner, A. L., and Randolph, T. W. (2000) The excluding effects of

sucrose on a protein chemical degradation pathway: methionine oxidation in subtilisin, *Arch. Biochem. Biophys. 384*, 123−132.
6. Lu, H. S., Fausset, P. R., Narhi, L. O., Horan, T., Shinagawa, K., Shimamoto, G., and Boones, T. C. (1999) Chemical modification and site-directed mutagenesis of methionine residues in recombinant human granulocyte colony-stimulating factor: effect on stability and biological activity, *Arch. Biochem. Biophys. 362*, 1−11.
7. Wood, M. J., Helena Prieto, J., and Komives, E. A. (2005) Structural and functional consequences of methionine oxidation in thrombodulin, *Biochim. Biophys. Acta 1703*, 141−147.
8. Stadtman, E. R., and Oliver, C. N. (1991) Metal-catalyzed oxidation of proteins. Physiological consequences, *J. Biol. Chem. 266*, 2005−2008.
9. Stadtman, E. R. (1992) Protein oxidation and aging, *Science 257*, 1220−1224.
10. Merker, K., Sitte, N., and Grune, T. (2000) Hydrogen peroxide-mediated protein oxidation in young and old human MRC-5 fibroblasts, *Arch. Biochem. Biophys. 375*, 50−54.
11. Kornfelt, T., Persson, E., and Palm, L. (1999) Oxidation of methionine residues in coagulation factor VIIa, *Arch. Biochem. Biophys. 363*, 43−54.
12. Liu, J. L., Lu, K. V., Eris, T., Katta, V., Westcott, K. R., Narhi, L. O., and Lu, H. S. (1998) In vitro methionine oxidation of recombinant human leptin, *Pharm. Res. 15*, 632−640.
13. Requena, J. R., Dimitrova, M. N., Legname, G., Teijeira, S., Prusiner, S. B., and Levine, R. L. (2004) Oxidation of methionine residues in the prion protein by hydrogen peroxide, *Arch. Biochem. Biophys. 432*, 188−195.
14. Chu, J. W., Yin, J., Wang, D. I.C., and Trout, B. L. (2004) Molecular dynamics simulations and oxidation rates of methionine residues of granulocyte colony stimulating factor at different pH values, *Biochemistry 43*, 1019−1029.
15. Fransson, J., Florin-Robertsson, E., Axelsson, K., and Nyhlen, C. (1996) Oxidation of human insulin-like growth factor 1 in formulation studies: kinetics of methionine oxidation in aqueous solution and in solid state, *Pharm. Res. 13*, 1252−1257.
16. Rosenberg, S., Barr, P. J., Najarian, R. C., and Hallewell, R. A. (1984) Synthesis in yeast of a functional oxidation-resistant mutant of human alpha-antitrypsin, *Nature 312*, 77−80.
17. Bott, R., Ultsch, M., Kossikoff, A., Graycar, T., Katz, B., and Power, S. (1988) The three-dimensional structure of Bacillus amyloliquefaciens subtilisin at 18 Å and an analysis of the structural consequences of peroxide inactivation, *J. Biol. Chem. 263*, 7895−7906.
18. Kim, Y. H., Berry, A. H., Spencer, D. S., and Stites, W. E. (2001) Comparing the effect on protein stability of methionine oxidation versus mutagenesis: steps toward engineering oxidative resistance in proteins, *Protein Eng. 14*, 343−347.
19. Stockman, B. J., Scahill, T. A., Roy, M., Ulrich, E. L., Strakalaitis, N. A., Brunner, D. P., Yem, A. W., and Deibel, M. R., Jr. (1992) Secondary structure and topology of interleukin-1 receptor antagonist protein determined by heteronuclear three-dimensional NMR spectroscopy, *Biochemistry 31*, 5237−5245.
20. Vigers, G. P.A., Caffes, P., Evans, R. J., Thompsom, R. C., Eisenberg, S. P., and Brandhuber, B. J. (1994) X-ray structure of Interleukin-1 receptor antagonist, *J. Biol. Chem. 269*, 12874−12879.
21. Becktel, W. J., and Schellman, J. A. (1987) Protein stability curves, *Biopolymers 26*, 1859−1877.
22. Pace, C. N. (1986) Determination and analysis of Urea and Guanidine Hydrochloride denaturation curves. *Methods Enzymol. 131*, 266−280.
23. Pace, C. N. (1990) Measuring and increasing protein stability, *Trends Biotechnol. 8*, 93−98.
24. Raibekas, A. A., Bures, E. J., Siska, C. C., Kohno, T., Latypov, R. F., and Kerwin, B. A. (2005) Anion binding and controlled aggregation of human interleukin-1 receptor antagonist, *Biochemistry 44*, 9871−9879.
25. Myers, J. K., Pace, C. N., and Scholtz, J. M. (1995) Denaturant m-values and heat capacity changes: relation to changes in accessible surface areas of protein unfolding, *Protein Sci. 4*, 2138−2148.
26. Agashe, V. R., and Udgaonkar, J. B. (1995) Thermodynamics of denaturation of Barstar: evidence of cold denaturation and evaluation of the interaction with guanidine hydrochloride, *Biochemistry 34*, 3286−3299.
27. Bongers, J., Cummings, J. J., Ebert, M. B., Federici, M. M., Gledhill, L., Gulati, D., Hilliard, G. M., Jones, B. H., Lee, K. R., Mozdzanowski, J., Naimoli, M., and Burman, S. (2000) Validation of a peptide mapping method for a therapeutic monoclonal antibody: what could we possibly learn about a method we have run 100 times, *J. Pharm. Biomed. Anal. 21*, 1099−1128.
28. Chen, B. L., and Schellman, J. A. (1989) Low-temperature unfolding of a mutant of phage *T4* lysozyme. 1- Equilibrium Studies, *Biochemistry 28*, 685−691.
29. Zhang, Y., Roy, S., Jones, L. S., Krishnan, S., Kerwin, A, B., Chang, B. S., Manning, M. C., Randolph, T. W., and Carpenter, J. F. (2004) Mechanism of benzyl alcohol induced aggregation of recombinant human interleukin-1 receptor antagonist in aqueous solution, *J. Pharm. Sci. 93*, 3076−3089.
30. Nicholson, E. M., and Scholtz, J. M. (1996) Conformational Stability of the Escherichia coli HPr protein: test of the linear extrapolation method and a thermodynamic characterization of cold denaturation, *Biochemistry 35*, 11369−11378.
31. Chiti, F., van Nuland, N. A., Taddei, N., Magherini, F., Stefani, M., Ramponi, G., and Dobson, C. M. (1998) Conformational stability of muscle acylphosphatase: the role of temperature, denaturant concentration and pH, *Biochemistry 37*, 1447−1455.
32. Hernandez, J. A., Meier, J., Barrera, F. N., de los Panos, O. R., Hurtado-, Gomez, E., Bes, M. T., Fillat, M. F., Peleato, M. L., Cavasotto, N. C., and Neira, J. L. (2005) The conformational stability and thermodynamics of Fur A (ferric uptake regulator) from Anabena sp. PCC 7119, *Biophys. J. 89*, 4188−4200.
33. Neira, J. L., and Gomez, J. (2004) The conformational stability of the streptomyces coelicolor histidine-phosphocarrier protein: characterization of cold denaturation and urea-protein interactions, *Eur. J. Biochem. 271*, 2165−2181.
34. Wong, H. J., Stathopulos, P. B., Bonner, J. M., Sawyer, M., and Meiering, E. M. (2004) Non-linear effects of temperature and urea on the thermodynamic and kinetics of folding and unfolding of hisactophilin, *J. Mol. Biol. 344*, 1089−1107.
35. Sheshadri, S., Lingaraju, G. M., and Varadarajan, R. (1999) Denaturant mediated unfolding of both native and molten globule states of maltose binding protein are accompanied by large ΔC_p's, *Protein Sci. 8*, 1689−1695.
36. Makhadatze, G. I., and Privalov, P. L. (1992) Protein interactions with urea and guanidinium chloride. A calorimetric study, *J. Mol. Biol. 226*, 491−505.
37. Zweifel, M. E., and Barrick, D. (2002) Relationships between the temperature dependence of solvent denaturation and denaturant dependence of protein stability curves, *Biophys. Chem. 101−102*, 221−237.
38. Roy, S., Katayama, D., Dong, A., Kerwin, B. A., Randolph, T. W., and Carpenter, J. F. (2006) Temperature dependence of benzyl alcohol and 8-anilinonapthalene 1- sulfonate aggregation of recombinant human interleukin-1 receptor antagonist, *Biochemistry 45*, 3898−911.
39. Carra, J. H., and Privalov, P. L. (1996) Thermodynamics of denaturation of staphylococcal nuclease mutants: an intermediate state in protein folding, *FASEB J. 10*, 67−74.
40. Khurana, R., and Udgaonkar, J. B. (1994) Equilibrium unfolding studies of barstar: evidence for an alternative conformation which resembles a molten globule, *Biochemistry 33*, 106−115.
41. Khurana, R., Hate, A. T., Nath, U., Udgaonkar, J. B. (1995) pH dependance of the stability of barstar to chemical and thermal denaturation, *Protein Sci. 4*, 1133−1144.
42. Koradi, R., Billeter, M., and Wüthrich, K. (1996) MOLMOL: a program for display and analysis of macromolecular structures, *J. Mol. Graphics 14*, 51−55.

BI700321G